Resource

Cell

Genome-wide Analysis of the Host Intracellular Network that Regulates Survival of *Mycobacterium tuberculosis*

Dhiraj Kumar,[1] Lekha Nath,[1] Md. Azhar Kamal,[1] Ankur Varshney,[1] Avinash Jain,[1] Sarman Singh,[2] and Kanury V.S. Rao[1,*]
[1]Immunology Group, International Centre for Genetic Engineering and Biotechnology, Aruna Asaf Ali Marg, New Delhi 110067, India
[2]Division of Clinical Microbiology, Department of Laboratory Medicine, All India Institute of Medical Sciences, Ansari Nagar, New Delhi 110029, India
*Correspondence: kanury@icgeb.res.in
DOI 10.1016/j.cell.2010.02.012

SUMMARY

We performed a genome-wide siRNA screen to identify host factors that regulated pathogen load in human macrophages infected with a virulent strain of *Mycobacterium tuberculosis*. Iterative rounds of confirmation, followed by validation, identified 275 such molecules that were all found to functionally associate with each other through a dense network of interactions. This network then yielded to a molecular description of the host cell functional modules that were both engaged and perturbed by the pathogen. Importantly, a subscreen against a panel of field isolates revealed that the molecular composition of the host interface varied with both genotype and the phenotypic properties of the pathogen. An analysis of these differences, however, permitted identification of those host factors that were invariantly involved, regardless of the diversification in adaptive mechanisms employed by the pathogen. Interestingly, these factors were found to predominantly function through the regulation of autophagy.

INTRODUCTION

Tuberculosis continues to prevail as the major cause of mortality around the world, despite implementation of control programs and the availability of effective drugs. The causative agent, *Mycobacterium tuberculosis* (Mtb), is an obligate human pathogen that primarily targets macrophages. After infection, intracellular mycobacteria are predominantly distributed between the early and late phagosomal compartments, with some also escaping into the cytoplasm (van der Wel et al., 2007). Their survival in the hostile intracellular milieu is facilitated through the dynamic modulation of a range of cellular processes. These include inhibition of pathways involved in the fusion of the phagosome with lysozomes, antigen presentation, apoptosis, and the activation of bactericidal responses (Koul et al., 2004). In addition, manipulation of the host cellular machinery also provides for access to essential nutrients (Pandey and Sassetti, 2008; Schaible and Kaufmann, 2005). While this pervasive influence clearly supports that the pathogen engages the molecular components of the cell in a broad network of interactions (Young et al., 2008), the details of this network are yet incomplete. In this connection, mycobacterial interference with the host signaling machinery has been extensively studied and pathways that are attenuated to enable the infection have been defined. The focus of these investigations, however, has been primarily restricted to events regulating pathogen entry and subsequent endocytosis (Koul et al., 2004; Vergne et al., 2004). The larger issue of mechanisms that mediate stabilization of the infection has remained unexplored.

To identify host factors regulating an established infection, we performed a genome-wide siRNA screen against host proteins in human cells that were first infected with a virulent strain of Mtb. Several host factors were identified whose expression levels proved critical for maintenance of the intracellular pathogen load. An analysis of these targets with their functional associations yielded a comprehensive description of the host molecular interface, and its constituent functional modules, that involved in crosstalk with the intracellular pathogen. By employing a panel of diverse field isolates, we also probed how this interface responded to the broad diversification in mechanisms of pathogenesis that Mtb exhibits in the human population. Surprisingly, the host determinants of intracellular pathogen load varied significantly across the isolates, suggesting that the clade identity of Mtb has an important bearing on defining its host factor dependencies. Nonetheless, by integrating the results, we could extract the obligate—host-specified—survival axis that was independent of the adaptive variations that the pathogen exploits in the field. Interestingly, this axis was largely comprised of members that regulated the process of autophagy.

RESULTS

Identification of Host Proteins that Regulate Mtb in Human Macrophages

We employed the SMARTPool human whole-genome small interfering RNA (siRNA) library to target a total of 18,174 genes as a mixture of four siRNAs per target gene. Human macrophage-like THP-1 cells were first infected with H37Rv and then

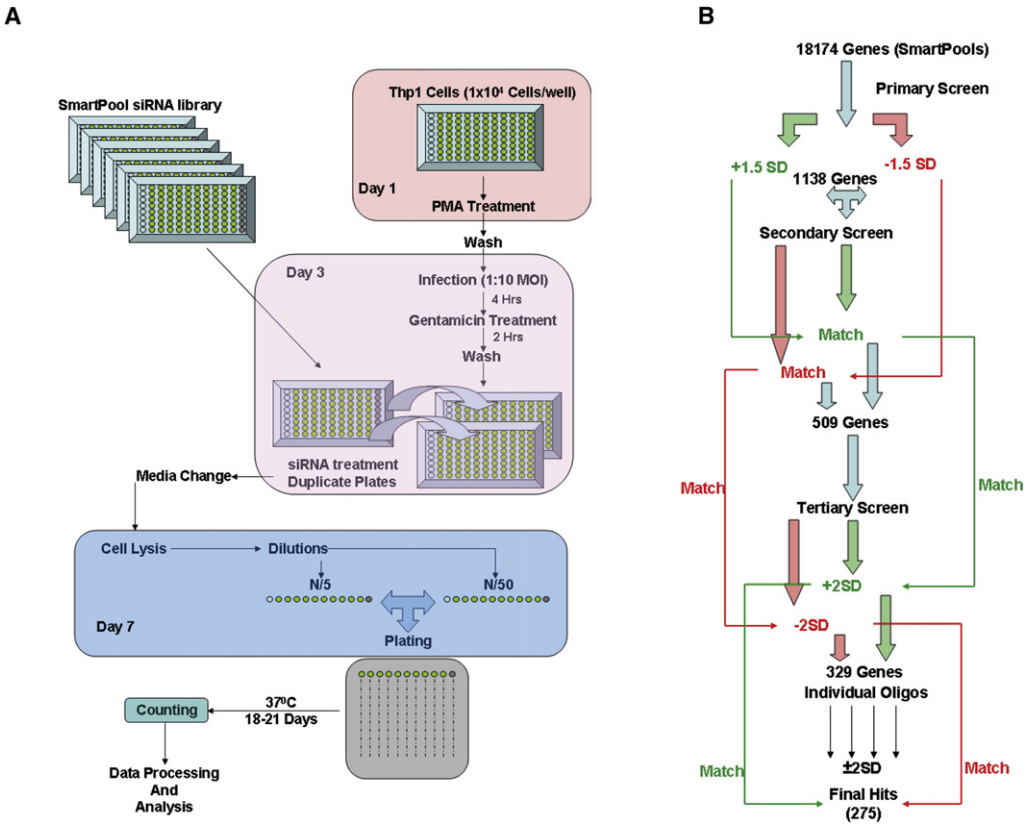

Figure 1. An Outline of the Protocol Employed for the siRNA Screen and Data Analysis

(A) The individual steps employed in our screening procedure are illustrated.

(B) The results obtained at each stage of the screen are summarized in the form of a flow diagram. The criterion used for selection at each stage is also indicated. See also Figure S1.

transfected with individual, target-specific, siRNA (Figure 1A and Figure S1 available online). This protocol ensured that interaction of Mtb with the target cell and its subsequent uptake through the endocytic pathway were unhindered. Consequently, our screen selected for those host factors that were involved in the regulation of an established infection. The effect of siRNA treatment on the intracellular mycobacterial load was determined from subsequently generated cell lysates, in terms of the colony forming units (CFUs) obtained.

The primary screen identified 1138 target proteins in which silencing led to either an increase, or a decrease, in mycobacterial CFU values that was greater than 1.5 standard deviations (SD) from the mean. A secondary screen further shortlisted on the basis of reproducibility of results, and the resulting 509 targets were then subjected to a tertiary screen in which only those siRNA pools in which the change in CFU value was greater than 2 SD of the mean CFU value obtained for the control wells were selected (Figure 1B). This iterative procedure (see the Extended Experimental Procedures) short-listed 329 siRNA pools (Table S1A). To next filter out "off-target" effects of siRNA, we rescreened the four siRNAs from each of the 329 target-specific pools separately to determine the number of individual siRNAs from each pool that retained a positive score (i.e., >2 SD of mean control value). For 106 of these, all of the four individual siRNAs scored positive, whereas for 88 pools this number was three. Further, two of the four individual siRNAs in 81 pools produced a significant effect, whereas this was true for only one siRNA in an additional set of 19 pools. For the remaining 35 pools, however, none of the individual siRNAs gave a positive result, thus identifying this latter group as clear false positives (Table S1B). We only took as validated those cases in which the results with the parent pool were reproduced by at least two of its constituent siRNAs, thus yielding a short list of 275 siRNA pools (Figure 1B and Table S1B). Of these, silencing with 270 led to a significant reduction in the intracellular mycobacterial load, while that with the remaining five pools yielded an enhanced CFU count (Figure 2A). A subsequent microarray analysis of the gene expression profile in uninfected THP-1 cells confirmed basal expression of the gene targets of all of these 275 siRNA (Table S2). These target proteins and their known functions are described in Table S3.

To verify whether any of the observed effects of these siRNA pools derived from an influence on cell viability, we treated uninfected cells with the validated siRNA pools and, after propidium iodide staining, measured the population with sub-G1 levels of DNA by flow cytometry. A comparison between the frequency of dead/apoptotic cells and the magnitude of the effect on Mtb CFU, obtained for each siRNA, revealed limited effects on cell

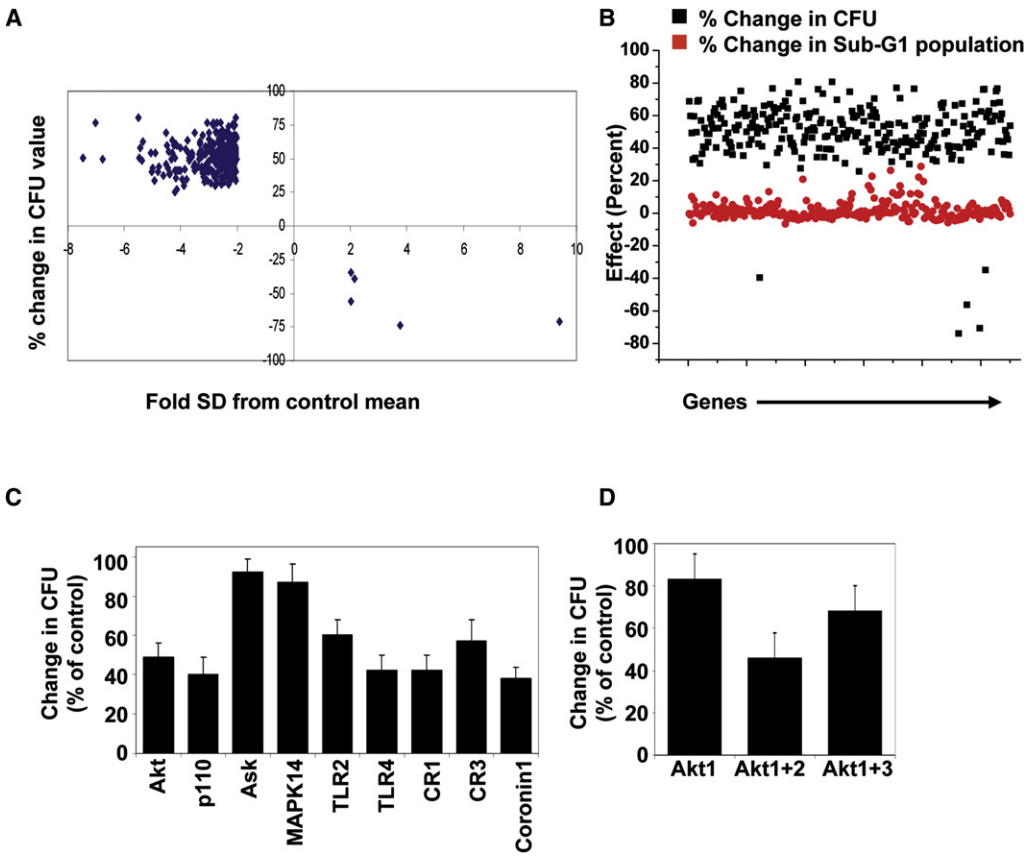

Figure 2. Validation of Targets Obtained from the Tertiary Screen

(A) The distribution of the top-scoring individual siRNAs obtained for the final list of targets (275) in our validation screen is shown. The x axis describes the fold change in CFU counts, from the standard deviation (SD) of the mean value for control wells. On the y axis, this change in CFU value, induced by a given siRNA, is expressed as a percent of the mean value for the corresponding control wells. In the latter, a positive value describes a decrease in bacterial load, whereas a negative value indicates an increase in CFU counts, relative to the control values.

(B) The effect of siRNA treatment on CFU versus that on induction of apoptosis in uninfected cells is compared as described in the main text.

(C) THP-1 cells were first treated with siRNA pools targeting the indicated molecules and then infected with H37Rv 36h later. The resultant CFU values (mean ± SD) are expressed as a percent of that obtained in GFP-silenced cells.

(D) The effects of silencing either Akt1 alone or in combination with either Akt2 or Akt3 in infected THP-1 cells are shown here. The percent of apoptotic cells obtained in each case were 18 ± 5, 26 ± 4, and 30 ± 7, respectively. In these experiments, individual silencing of either Akt2 or Akt3 did not yield any significant effect on Mtb CFU (<20%).

See also Figure S2.

apoptosis in comparison with the more wide-ranging effects on Mtb levels (Figure 2B). Similar results were also obtained using an MTT assay (Figure S2), further confirming that the effect of these siRNAs was not due to toxic effects on the host cells. This stability of uninfected cells to siRNA treatment is consistent with our observation that PMA-differentiated THP-1 cells were more resistant than cycling cells to the depletion of key survival-related molecules (Figure S2).

Factors Influencing Results of the siRNA Screen

The host factors identified to regulate Mtb infection by our screen showed a poor concordance with those implicated in previous studies (see Table S1). However, while these earlier studies had largely concentrated on events occurring either during or soon after the uptake of pathogen by the host macrophage (Koul et al., 2004), our screen investigated a later time window involving the establishment of a sustainable equilibrium with the host intracellular milieu. Therefore, to verify whether the stage of infection examined had any bearing on outcome, we selected a panel of nine targets that, though known to regulate the early processes after Mtb uptake, were not identified in our screen. The effects of silencing expression of these molecules either during or subsequent to the exposure of cells to H37Rv were then compared. Intracellular Mtb loads were significantly reduced in seven of these cases when the target proteins were depleted at the time of infection (Figure 2C). However, postinfection silencing again had no significant effect. Further, in these latter experiments, a significant inhibitory effect of Akt1 was only observed when its silencing was combined with that of its isoform, Akt2 (Figure 2D). Thus, temporally distinct stages of the infection are also characterized by distinctions in the regulatory host factors involved. Consequently, the targets identified

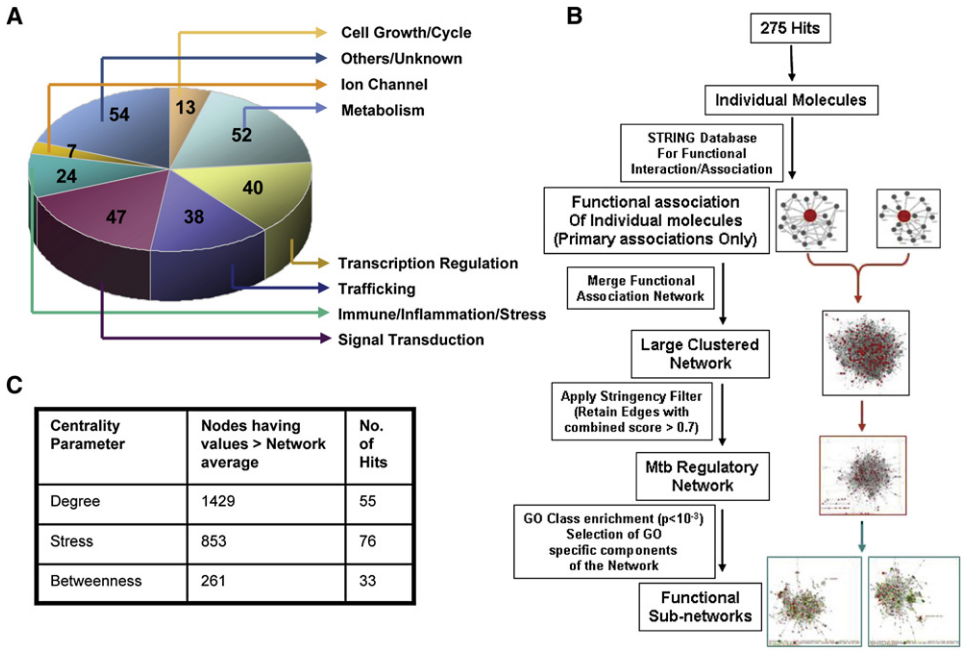

C

Centrality Parameter	Nodes having values > Network average	No. of Hits
Degree	1429	55
Stress	853	76
Betweenness	261	33

D

Network	Avg. Clustering Coefficient	Avg. Path Length	Avg. Node Degree
Mtb RN	.526	3.99	21.66
Metabolism	.494	3.9	17.839
ST	.493	3.304	18.81
Im/St	.388	3.358	11.068
Traffic	.449	4.059	10.803
TF	.457	3.346	20.809
CCR	.448	3.145	14.889

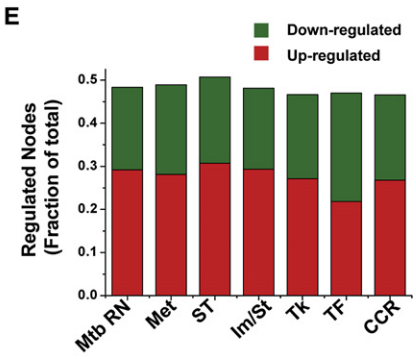

Figure 3. Functional Classification of the "Hits" and Extraction of the Mtb-Regulatory Network

(A) The pie chart shows the distribution of the 275 validated targets between eight broad classes of physiological functions.

(B) The Mtb-regulatory network was constructed with the steps outlined here, which also include the procedure involved in extracting the GO enriched subnetworks.

(C) Analysis of the Mtb-regulatory network for the indicated centrality parameters with the "network analyzer" plugin in Cytoscape. For each parameter, nodes having a value higher than the network average are considered more important for that particular function.

(D) Comparison of the intrinsic network parameters between the individual subnetworks and the parent Mtb-regulatory network.

(E) Estimation of the fraction of the total number of nodes, in either the parent network or its component modules, whose genes were either up- or downregulated as a result of infection of cells with H37Rv.

by our screen were likely those whose roles either persisted or were initiated during the later stages of the infection. However, these results notwithstanding, both insufficient silencing of the target and reversibility of the silencing effect over the time course of our experiment could be expected to contribute toward false negatives in our screen.

Extraction and Analysis of the Host Cell-Specific Mtb-Regulatory Network

To further characterize the host molecules identified, we employed their Gene Ontology (GO) class descriptions to classify them under eight broad categories of cellular function. These categories and the distribution of the 275 host factors between them are described in Figure 3A and Table S3. Barring molecules with either unknown or inadequately characterized function, it was the functional categories of metabolism, signal transduction, transcription regulation, and trafficking that were predominantly represented, collectively accounting for nearly 65% of all of the "hits" (Figure 3A). Next, to define the host molecular interface involved in interactions with the pathogen, we extracted the cellular network that was composed of all the validated siRNA targets. For this we sourced the STRING database to determine the functionally associated partners for each of the target molecules, and these interactions were then merged together to generate the network (see Figure 3B). The resulting network, termed as the Mtb-regulatory network, was comprised of 4771

nodes and 51,677 edges (interactions) (Tables S5 and S6). A clustering coefficient (CC) of 0.526 was obtained, which is consistent with a "small-world" architecture that facilitates easy information flow between the component nodes (Barabási and Oltvai, 2004). A randomization of this network through 100 iterations where links were arbitrarily shuffled without altering their number resulted in a 20-fold reduction in the clustering coefficient (0.03 ± 0.0007), with a concomitant reduction also in the mean path length (from 4.0 to 2.8 ± 0.003). Thus, the topological features of the Mtb-regulatory network were not randomly derived, but rather represent unique properties. Additionally, the low frequency of our "hits" among the nodes with a higher than average value for the measured centrality parameters also reiterated that this network was not biased toward the siRNA-identified targets (Figure 3C, Table S6).

Modular Composition of the Mtb-Regulatory Network

We further dissected the Mtb-regulatory network to examine its constituent functional modules. With the exception of ion channel-related activities, the other functional groups described in Figure 3A were identified to form discrete subnetworks that were significantly overrepresented ($p < 10^{-3}$). The subnetworks obtained for each of these GO classes are depicted in Table S6, and the two most enriched ones were those for the functions of metabolism and signal transduction. This is consistent with the fact that, in addition to sourcing nutrients, intracellular survival of Mtb requires the pathogen to modulate multiple host cellular functions that are under the regulatory control of the signaling machinery (Schaible and Kaufmann, 2005; Warner and Mizrahi, 2007). Similarly, the relatively large size of the module corresponding to the host cell transcription regulatory network is also in keeping with earlier findings that infection causes extensive alterations in the host cell transcriptome (Nau et al., 2002).

A comparison of the intrinsic network properties of the individual subnetworks with that of the parent Mtb-regulatory network revealed that these parameters were only slightly affected (Figure 3D). Additionally, the parent network and its subnetworks all displayed a broad distribution in node degree (Table S6), confirming the modular organization of the Mtb-regulatory network.

Coexpressing Modules within the Functional Subnetworks Highlight the Dynamic Features of Host-Pathogen Interactions

To explore how the above functional modules were perturbed by the pathogen, we analyzed the gene expression profile of THP-1 cells at various times after infection with H37Rv. These results were then integrated into the above functional-class subnetworks to determine the relative expression patterns of the nodes within each module. Interestingly, expression of nearly half of the genes coding for the nodes in each of these modules was either up- or downregulated (Figure 3E), suggesting that the functional properties of the modules were significantly altered as a result of the infection. Next, we segregated the coregulated clusters within each subnetwork (see Table S6). Taking each of these clusters, we then searched for connected modules that were composed of a minimum of three nodes. Interestingly, this exercise revealed the existence of a large, highly connected module, along with a few smaller clusters, within each of the functional subnetworks. Further, these coexpressing modules also included several of the targets identified by our siRNA screen. The largest up- and downregulated module from select subnetworks is shown in Figure 4, and the complete sets are presented in Table S7.

Intriguingly, the subnetworks representing the GO classes of immunity/inflammation/stress, transcription regulation (Figure 4), signal transduction, metabolism, and cell cycle/growth all included a functional cluster of upregulated genes that was centered on the serine/threonine kinase Akt. While this reaffirms the importance of this group of kinases in regulating Mtb levels (Kuijl et al., 2007), these results also provide a resolution of the multivariate pathways through which Akt/PKB may act, in regulating the intracellular infection. The presence of a cluster within the metabolism subnetwork that was centered on ACSL1—an identified siRNA target—was also of interest (Figure 4). Mycobacterial lipid metabolism is central to its virulent properties, and coupled lipid metabolism between host and the pathogen plays a role in mycobacterial survival and virulence in host cells (Jain et al., 2007). Interestingly, however, ASCL1 has also been implicated in the etiology of diabetes (Gertow et al., 2004). The ASCL1-focused cluster identified here may, therefore, help to gain mechanistic insights into the close association observed between diabetes and susceptibility to tuberculosis (Kaufmann et al., 2005).

The coregulated clusters identified within the immune/inflammation/stress subnetwork also provide the blueprint for an understanding of how the pathogen modulates the innate and adaptive components of the host immune response. Thus, the upregulated cluster shown in Figure 4 (and Table S7) primarily includes nodes that are immunosuppressive (IL-10, CTLA4, BTLA), are involved in the induction of apoptosis of T cells (FASLG, PDCD1LG2, TRAF6, NOD1), or bias toward a Th2 response (IL-4, GATA3). TLR8—a hit in our screen—is another node of particular interest here. Genetic variants of this protein have recently been linked to susceptibility to pulmonary tuberculosis (Davila et al., 2008). In contrast to the upregulated cluster, the downregulated cluster of nodes from the immune/inflammation subnetwork included both extracellular (IL-1B, IL-7, 1L-27, IL-6, IFNB1, CXCL5, CCL11, CXCL14, etc.) and intracellular/cellular (EBI3, IRAK2, IRF-4, NOD2, MYD88, CSF2, NOTCH 1 and 4, etc.) mediators of an inflammatory response. This is consistent with the known immune-evasive strategies adopted by virulent mycobacteria within the host (Flynn and Chan, 2001).

Thus, our sequential analysis involving the incorporation of targets identified by the siRNA screen into a functional association network, then resolving this network into distinct GO-based subnetworks, and finally integrating into these the results from microarray experiments allowed us distinguish those modules that were specifically influenced by the infection. These coregulated clusters likely represent dynamic expressions of the interplay between the pathogen and the molecular components of the host cellular machinery. A more detailed analysis of these clusters, along with those involving host factors whose expression levels remain unchanged (see Table S7) would, however,

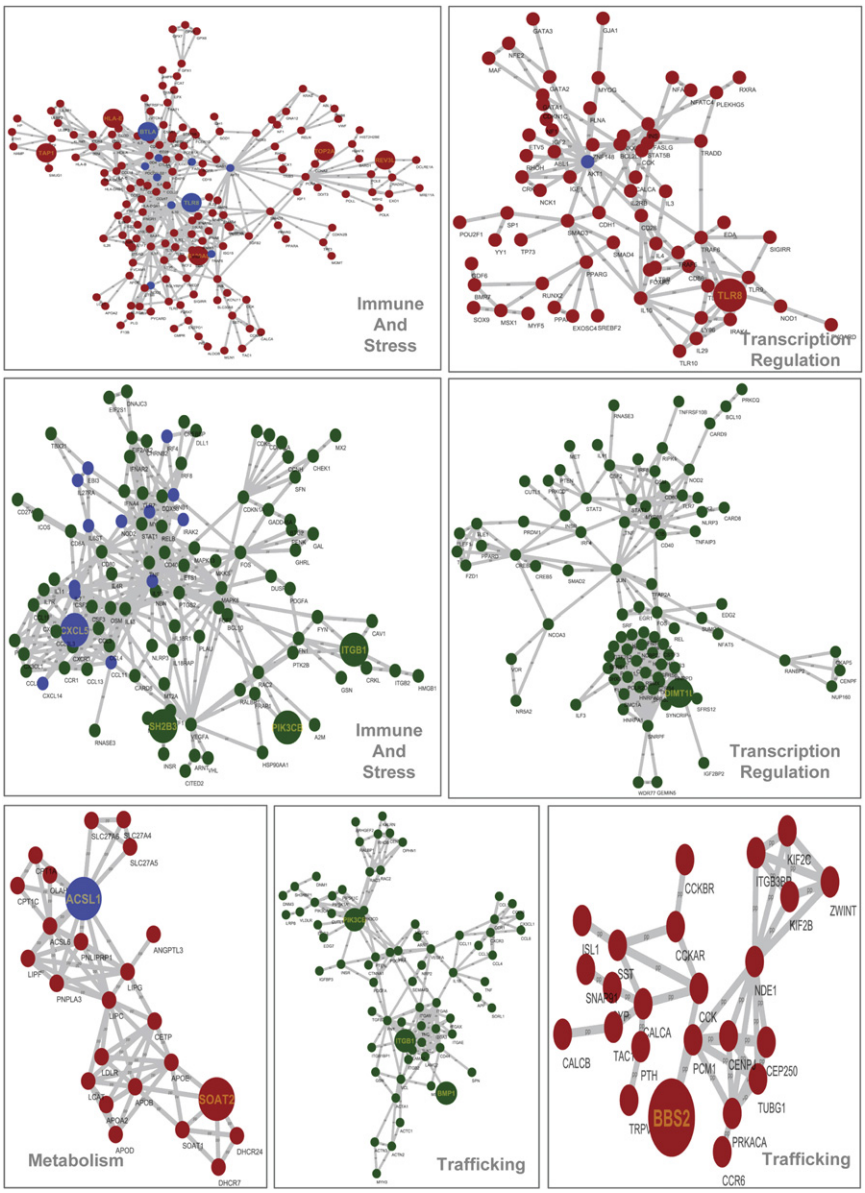

Figure 4. Identification of Coexpressing Modules within the Functional Subnetworks

Figure shows the largest coexpressing clusters from select functional subnetworks identified in Figure 3. Clusters shown in red are upregulated and those in green downregulated after infection of THP-1 cells with H37Rv. The slope for each gene, from a plot of the expression data at various time points, was calculated to group the up- and downregulated nodes. Genes with a slope higher than 0.15 were considered to be upregulated, and those with a slope lower than −0.15 were taken as being downregulated. Nodes in bold with names in yellow are from our list of validated targets from the screening data, and the nodes referred to in the text are highlighted in blue. See also Table S7.

be required before more definitive interpretations can be made on host factor-dependent regulation of the pathogen.

Defining a Filtration Window by Using a Panel of Mtb Clinical Isolates

Mtb exhibits a broad spectrum of genotypic and phenotypic diversification in the human population. To date, at least six main lineages and 15 sublineages of this pathogen have been described (Brudey et al., 2006; Gagneux et al., 2006). Further, the clinical presentation of this infection can dynamically shift between states of latent, persistent, and active infection in which the pathogen can again potentially display a spectrum of phenotypic variations that extend from drug-sensitive to multiple-drug (MDR-Mtb), and even extensive drug, resistance (Ginsberg and Spigelman, 2007). It is, however, unknown whether such variations also involve alterations in the mechanisms that support intracellular survival of the pathogen.

To explore this, we extended our studies to include a panel of seven independent field isolates of Mtb that collectively represented a range of phenotypic and genotypic variations. For example, these isolates displayed distinct patterns of drug resistance against the four frontline drugs used for the treatment of tuberculosis (Figure 5A). While three of these isolates belonged to the class of MDR-Mtb, exhibiting resistance to any three of these four drugs, the resistance profile describing each isolate differed from that of the other two. The remaining four isolates were also similarly distinguished in that they were each resistant to just a single drug, but again in a manner that was exclusive of the other isolates in this subgroup (Figure 5A). In addition to drug-sensitivity profiles, these Mtb isolates also defined a heterogeneous group of genotypes, collectively representing four distinct lineages (Figure 5A and Figure S3).

The isolates also displayed diverse growth properties in THP-1 cells, with apparent growth rates that were either significantly higher (JAL2287) or lower than that of H37Rv (Figure 5B). Importantly, this variation was specific to infected cells since these isolates demonstrated broadly comparable growth rates in extracellular cultures (Figure 5C). Although differences in apparent growth rates presumably reflect differences in the balance achieved between mycobacterial replication and killing, differences in intracellular rates of accumulation in THP-1 cells have been shown to correlate with epidemiological evidence for strain virulence (Park et al., 2006; Theus et al., 2006). Thus, variations in the apparent growth rates seen in Figure 5B also imply variations in the in vivo virulence properties of these

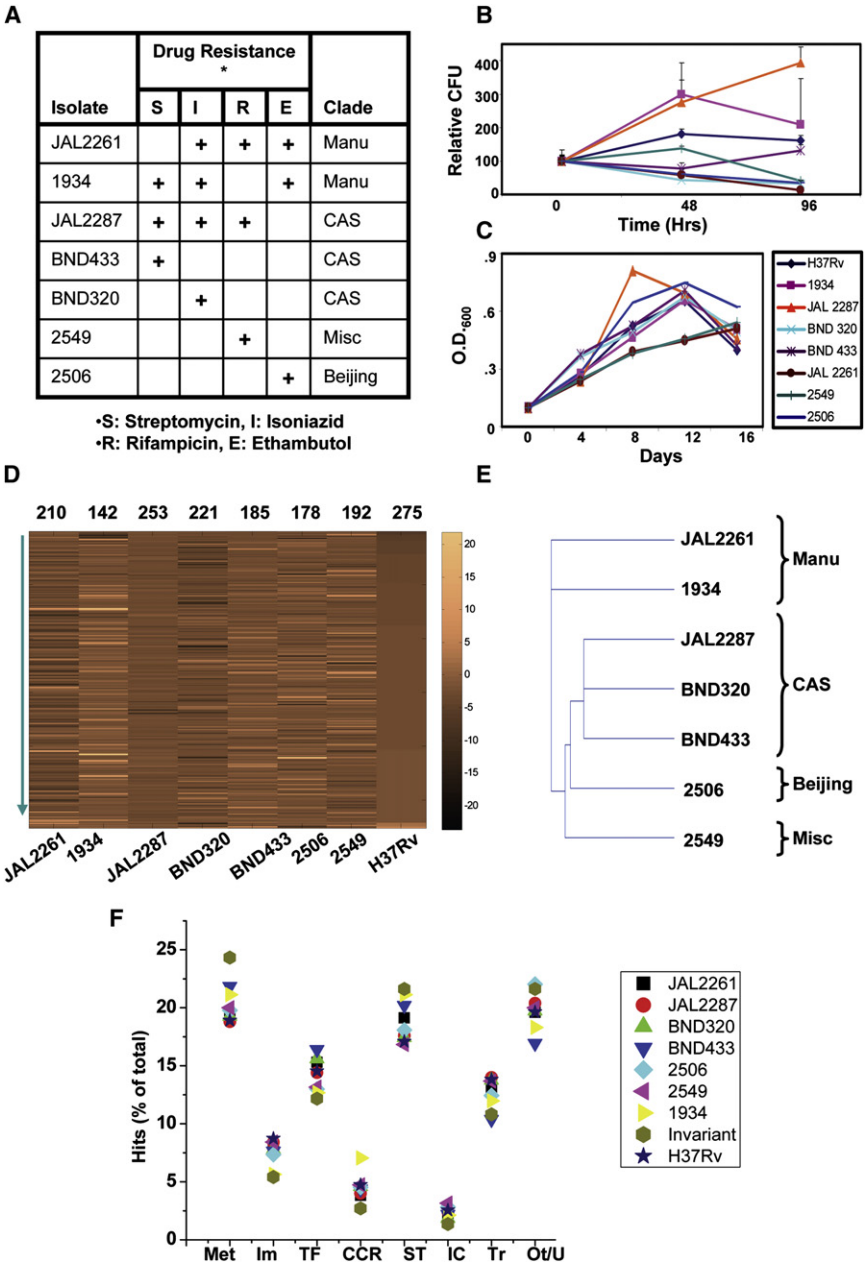

Figure 5. Diverse Field Isolates of *Mycobacterium tuberculosis* Exhibit Heterogeneity in Terms of Host Factor Recruitment

(A) The drug-resistance patterns and the clade identity of the field isolates are given here. A "+" denotes resistance to the corresponding drug. H37Rv is sensitive to all of these drugs.

(B) Growth properties of the individual isolates in infected THP-1 cells. CFU values, expressed as a function of viable host cells, obtained at the indicated times after infection, are shown. Data are the mean (± SD) of three separate experiments. p values for the significance of differences in CFU values for the isolates from that of H37Rv at the 96 hr time point ranged from 0.02 to 0.05 in all cases, except for 1934, where it was 0.8.

(C) Extracellular growth properties of the individual isolates. Mycobacteria were grown in Middlebrock 7H9 media, and the optical density (OD; 600 nm) obtained at the indicated times is shown.

(D) Comparison of results from the screen of THP-1 cells individually infected with the seven clinical strains. The siRNAs against the 275 genes validated in H37Rv-infected cells were employed here, and the numbers on the top of each column represent the number of validated hits obtained in each case. The magnitude of the effect is given in terms of the fold change in SD value from the mean of the control wells and is indicated by the color bar. Values are the mean of two separate experiments, which were performed exactly as described for H37Rv.

(E) A cluster analysis of the strains on the basis of their sensitivity to the 275 host factors.

(F) Shown here is the percent distribution of strain-specific hits among the eight broad functional classes described. These functional classes are metabolism (Met), immune/inflammation/stress (Im), transcription regulation (TF), cell growth/cycle (CCR), signal transduction (ST), ion channel (IC), trafficking (Tr), and those with presently unknown or inadequately characterized function (Ot/U). Results for the subset of 74 host proteins that served as a common requirement for all the Mtb strains tested are also included (Invariant). See also Figure S3.

strains. Cumulatively, then, the panel of Mtb isolates described in Figure 5A presents a composite reflection of the Mtb strain diversification observed in the field.

Mtb Exhibits Strain-Specific Variations in Dependence on the Host Cellular Machinery

We next took the validated siRNA pools described in Figure 2A and screened against THP-1 cells separately infected with each of the Mtb isolates in Figure 5A. The results we obtained, after employing a cutoff of >2 SD of the control mean, are described in Table S8 and illustrated in Figure 5D. It is apparent here that not all of the 275 targets validated against H37Rv were equally effective against the other strains tested. Particularly striking, however, was that even among the field isolates, both the number and spectrum of effective targets varied quite distinctly. Although there were significant overlaps, no two isolates yielded an identical profile of sensitivities to the siRNA pools tested (Figure 5D and Table S8).

To further analyze these results, we calculated the similarity index using the paired group algorithm for measuring the constrained Euclidean similarity coefficient, and the resulting dendrogram is presented in Figure 5E. As shown, isolates of the CAS lineage—JAL2287, BND320, and BND433—formed a cluster of similarly responding strains to the siRNA pools tested. Similarly, the two most distantly placed strains in terms of similarity index were the Manu clade isolates JAL2261 and 1934;

whereas the remaining strains 2506 (Beijing) and 2549 (Miscellaneous) were located in between these two extreme groups (Figure 5E). Thus, distinctions in clade identity appear to serve as the primary determinant for the observed differences in the spectrum of host molecules recruited in Figure 5D. However, differences in phenotypic properties such as replication rates are also likely to contribute toward these distinctions. Notably, the strain-specific variations seen here also raise the possibility that at least some of these isolates may exhibit dependencies on host factors that are redundant in the context of H37Rv infection. Such factors would be missed in our present study.

Identifying the Mtb Strain-Independent Regulatory Axis of the Host Cell

A closer inspection of Figure 5D revealed that, in spite of the differences, 74 of the siRNA pools were commonly effective in reducing intracellular loads of all the strains tested. That is, the host factors targeted by these siRNA pools were invariantly required regardless of drug resistance profile, virulence properties, and clade identity (listed in Table S9). To examine the nature of similarities and distinctions in host factor dependencies between these Mtb isolates, we probed for any alterations in bias toward the host cellular functional modules. Interestingly, the percent distribution of the "hits" for each strain—including H37Rv—among the functional groups described in Figure 3A remained constant, indicating that the relative extent of utilization of the different functional modules of the host cell was unchanged across these strains (Figure 5F). This was equally true for the 74 protein targets that were invariantly involved for all the strains (Figure 5F), supporting the relevance of each of these functional classes in regulating intracellular Mtb levels.

The Mtb Strain-Independent Regulatory Axis Functions by Regulating Autophagy

Recent experiments have demonstrated that stimulation of autophagy (or, xenophagy) in infected macrophages, either by physiological or pharmacological means, severely reduces viability of intracellular Mtb (Gutierrez et al., 2004; Levine and Deretic, 2007). Consistent with this, we also found that pharmacological activation of autophagy, at 48 hr after the infection, significantly reduced intracellular Mtb load in THP-1 cells (Figure 6A). Importantly, these results extended the earlier findings by establishing the susceptibility of Mtb to xenophagy during this later window of infection. We therefore asked whether the observed effects of depletion of at least some of the identified host targets, on Mtb survival, could in fact be mediated through the activation of xenophagic pathways. To test this, we subjected H37Rv-infected cells to siRNA-mediated silencing of each of the 74 host molecules that were identified as the strain-independent set of Mtb-regulatory factors in Figure 5D (and Table S9). After this, we determined whether the effects of target protein silencing on intracellular Mtb levels could be reversed by 3-methyladenine (3MA), the classical inhibitor of autophagy (Seglen and Gordon, 1982). By taking a 50% reversal of the effects of a given siRNA as the cutoff for significance, we found that inclusion of 3MA significantly attenuated the effects of 44 of the 74 target-specific siRNAs tested (Figure 6B, Table S9). This suggests that the Mtb-inhibitory effects that result from depletion of over half of the Mtb strain-independent regulatory factors identified by our screen are likely to be mediated through the induction of xenophagic pathways. The mechanism of action resulting from depletion of the remaining 30 targets, however, awaits clarification.

Although the antimicrobial properties of IFN-γ also derive in part from its ability to stimulate autophagy in host cells (MacMicking et al., 2003; Singh et al., 2006), Mtb-infected human macrophages are desensitized to activation by this cytokine (Ting et al., 1999). This desensitization facilitates persistence of the pathogen even in tuberculosis patients expressing high levels of IFN-γ in pleural fluid (Flynn, 1999). Consistent with this, stimulation of H37Rv-infected THP-1 cells with IFN-γ had only a marginal (<15%) affect on pathogen viability, although these cells continued to express high levels of the IFN-γ receptor (data not shown). Thus, attenuation of cytokine responsiveness of the host cell by Mtb also probably includes attenuation of IFN-γ-dependent activation of xenophagic pathways.

The 3MA-sensitive host factors identified in Figure 6B probably represent negative regulators of xenophagy since it was the silencing of expression of these molecules that induced suppression/elimination of intracellular Mtb. This could be experimentally verified by our subsequent findings that silencing of these 44 targets in infected cells resulted in an increase in levels of LC3-II - the marker for autophagosomes (Figure S4). Therefore, to determine how levels of the genes for these 44 proteins were influenced by Mtb infection, we reanalyzed our expression data (Figure 4). Thirteen of these were indeed upregulated after infection of THP-1 cells, whereas expression levels of the remainder were either unchanged (20), or suppressed (11) (Figure 6C). It is possible that select upregulation of only a small subset of these factors is sufficient to inhibit the autophagic response of the host cell. A similar explanation may also account for the results of our parallel examination of the public database (NCBI, GEO) for the expression levels of these 44 genes in macrophages stimulated with IFN-γ. Here again only some of these genes (19) were downregulated, with four of these being common to the group of genes induced by H37Rv infection (Figure 6C).

The poor overlap between the xenophagy-related genes suppressed by IFN-γ and those induced by H37Rv infection led us to explore whether the suppression of any one of these host factors would potentiate IFN-γ responsiveness of the infected host cell. We depleted the targets listed in Figure 6C in H37Rv-infected cells and then stimulated these cells with IFN-γ. The effect on intracellular Mtb load was then compared with that obtained in the absence of cytokine stimulation. Interestingly stimulation with IFN-γ resulted, in several instances, in an enhanced reduction in CFU that was at least 1.5-fold greater than that obtained in response to siRNA treatment alone (Figure 6D). Since IFN-γ alone had only a marginal influence (<15%), these results reveal the synergistic effect that can be achieved by combining the depletion of select xenophagy-related genes with cytokine stimulation.

Thus, activation of xenophagic pathways through the downmodulation of negative regulators in the host macrophage provides an effective mechanism for elimination of the intracellular Mtb in a strain-independent manner. Also significant is our

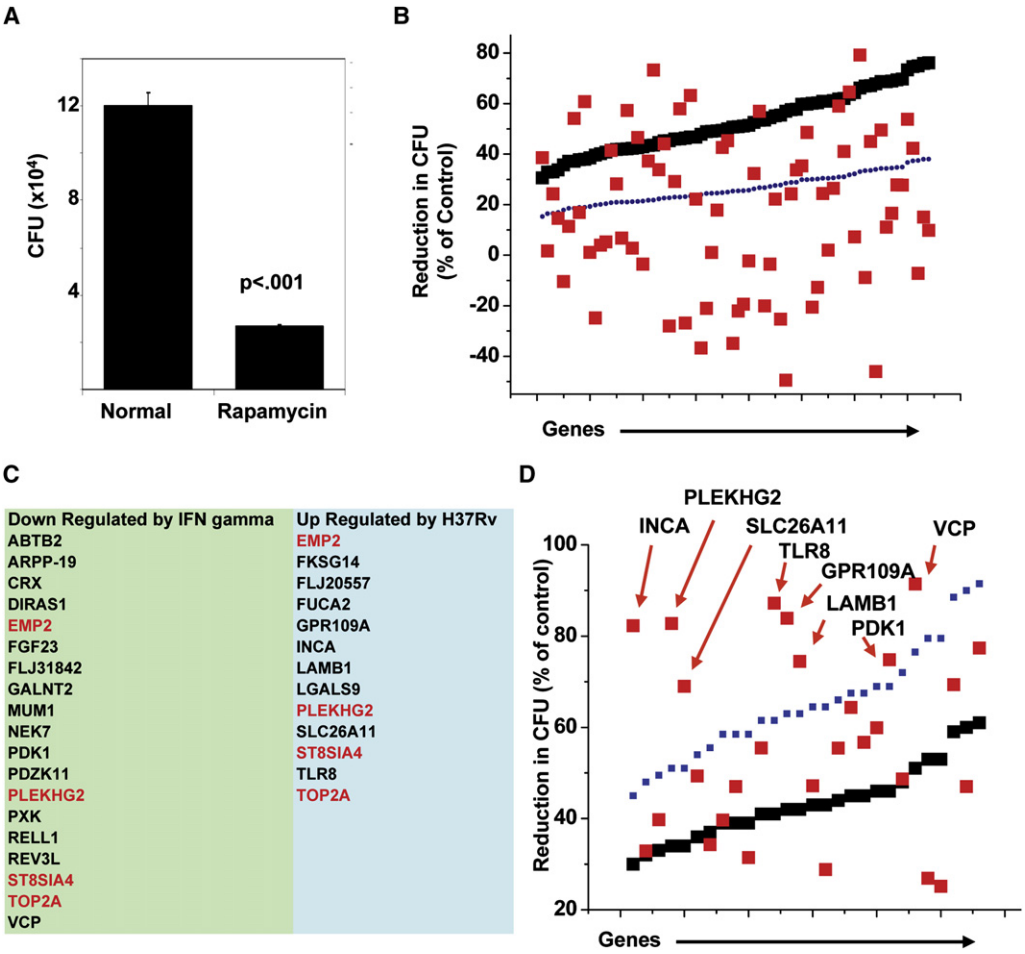

Figure 6. Intracellular Survival of Mtb Involves Inhibition of Xenophagic Pathways

(A) THP-1 cells infected with H37Rv were treated with rapamycin at 48 hr after infection and the resulting CFU counts were compared against that from untreated, but infected (Normal), cells. Values are the mean (±SD) of three separate experiments, and the percent of apoptotic cells obtained in rapamycin-treated cells was <18%.

(B) The extent of reduction in CFU values obtained in H37RV-infected cells treated with each of the 74 target-specific siRNA either in the absence (black squares) or presence (red squares) of 3MA are shown. 3MA (5 mM) was added at 36 hr after siRNA treatment, and values are the percent reduction in CFU counts from that obtained in infected cells treated with GFP-specific siRNA, in the absence of 3MA. The blue dashed line defines the threshold value of 50% of the inhibitory effect for each of the siRNA pools without 3MA treatment, and the red squares falling below this were considered to represent a significant attenuation of siRNA potency by 3MA treatment.

(C) List of the genes for the 44 3MA-sensitive targets whose expression levels were either downregulated by IFNγ treatment or upregulated by H37Rv infection. The four targets that are present in both sets are highlighted in red.

(D) H37Rv-infected cells were treated with siRNA against the 44 3MA-sensitive targets identified in (B). Subsequently (at 36 hr), parallel sets of these cells were either left unstimulated or stimulated with IFN-γ (20 ng/ml). Mycobacterial CFUs obtained after an additional culture period of 54 hr, both in the presence (red squares) and absence (black squares) of IFN-γ treatment, are shown. The cutoff representing a 1.5-fold increase in inhibition over that obtained for the siRNA treatment alone is depicted as the blue dashed line, and the target proteins showing cooperativity are identified.

See also Figure S4.

demonstration that suppression of some of these regulators can synergize with an IFN-γ stimulus to yield an enhanced suppression/elimination of the pathogen. While the mechanism involved is presently unknown, we believe that these latter findings are especially relevant from the standpoint of the developing new strategies for the therapy of tuberculosis. Thus, in vivo, the antimicrobial effects of pharmacological inhibitors of such molecules may potentially be further enhanced by the Th1 immune responses that are generated in response to the infection by the host.

The Survival versus Death Balance of Intracellular Mtb

Inside the host macrophage, multiple subcellular compartments provide a survival niche for Mtb (de Chastellier, 2009). Our present results indicate that survivability of the pathogen in either of these niches involves dependence on host factors that derive from multiple functional modules of the host cellular machinery. Figure 7A illustrates this and also highlights the multiplicity of cellular functions that Mtb is required to influence to ensure its survival. This dependence on diverse regulatory processes would then also provide a window of vulnerability where

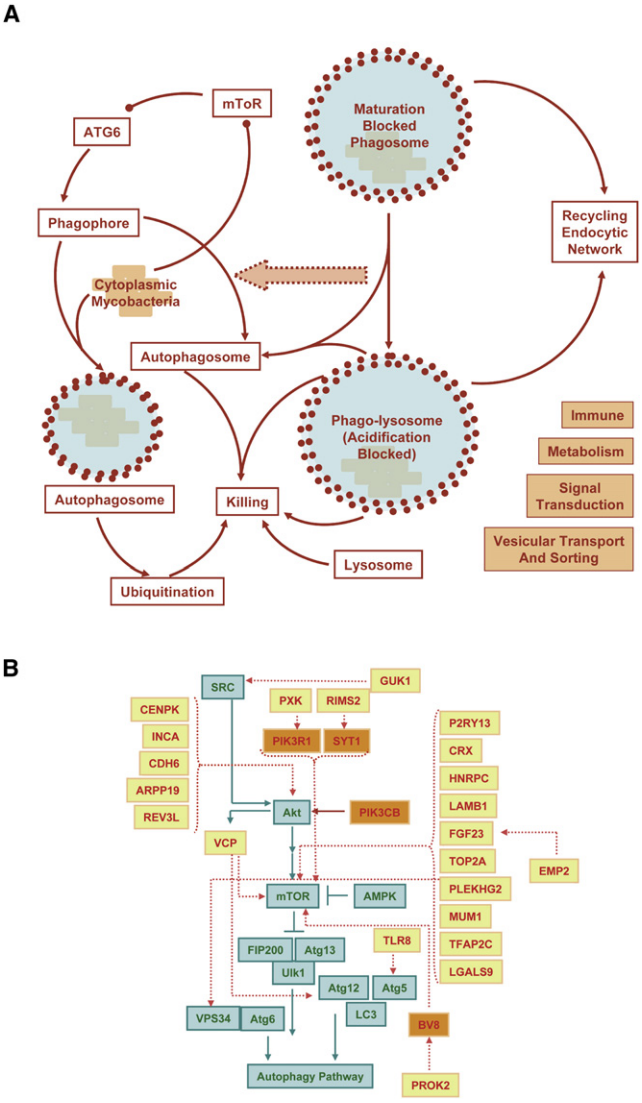

Figure 7. The Balance between Survival and Death for Intracellular Mtb

(A) An illustration of the microbicidal pathways initiated by the host macrophage and the counter-evasive strategies employed by the mycobacteria. After endocytic uptake, maturation of the phagosomes to yield acidified phagolysosomes constitutes an important microbicidal response of the host cell. Virulent mycobacteria, however, inhibit these processes and persist in recycling endocytic vesicles that have a relatively high pH. In addition to this, Mtb can also escape from these vesicles into the cytoplasm of the host cell, thereby accessing an alternate survival niche in the intracellular milieu. Autophagy provides another mechanism by which the host macrophage can potentially eliminate both intravesicular and cytoplasmic pools of the pathogen. Formation of the autophagosome is, however, effectively inhibited by virulent strains of Mtb, although the underlying mechanism is presently unknown. The figure illustrates these various pathways and the lower right segment of this panel indicates the functional modules of the macrophage that contribute toward regulation of autophagy.

(B) Plausible links between components of the relevant subset of the invariant host factors required for Mtb survival, with the known pathways for initiation of autophagy are shown here. These links were extracted through an analysis of the Mtb-regulatory network for shortest paths between the known autophagy effector molecules and the candidate genes identified here.

disruption of a key interaction (e.g., through the silencing of the host protein by siRNA) could well lead to a cascading effect that shifts the equilibrium in favor of the host cell.

Taking our results in Figure 6B, we generated a coarse map of the pathways that may mediate induction of Mtb-targeted xenophagy. To do this, we explored our Mtb-regulatory network (Tables S5 and S6) for associations between the 44 targets described to be 3MA sensitive and molecules involved in the initiation of autophagy (Fratti et al., 2003; Van Limbergen et al., 2009). We could link 22 of these genes with components of the autophagic machinery within a maximum path length of four (Table S10). Importantly, these results suggested that this subset of host Mtb-regulatory factors cumulatively act at multiple steps in the autophagy initiation pathway (Figure 7B). Thus, while some of these factors directly influence mTOR, others probably act either on the upstream signaling intermediates, or on processes mediating vesicle elongation (Figure 7B). Therefore, while Mtb may successfully manipulate the host cellular machinery to its survival advantage, the multilayered and multifaceted nature of host regulatory pathways involved provides a ready spectrum of molecules that can potentially be targeted to induce a release from this control.

DISCUSSION

Although cellular processes regulating the binding to and subsequent endocytosis of Mtb by macrophages have been characterized in detail, information on host factors that are implicated in regulating a stable infection is lacking (Monack et al., 2004). Therefore, our present screen was deliberately designed to investigate a window that was initiated several hours subsequent to mycobacterial uptake. This window presumably represents a phase in which the pathogen is either establishing or has established a sustainable equilibrium with the host intracellular milieu. Several host factors whose depletion significantly influenced the load of the intracellular pathogen could be consequently identified. Importantly, these proteins could be incorporated into a functional association network in which the component modules together defined the entire range of cellular processes that participate in the interplay between the host cell and the pathogen. At one level, this network provided a molecular-level description of the molecular constituents of the host cell that were engaged by the pathogen. In addition, as demonstrated in the case of Akt/PKB, the network also yielded clues on the multivariate nature of controls through which several key molecules may exercise their influence on the outcome of an infection process.

To capture the dynamic features of host-pathogen interactions, we integrated information on infection-induced alterations in the host cell transcriptome into the Mtb-regulatory network and then extracted coregulated clusters from the individual GO class-specific modules. The rationale here was that while our siRNA screen identified the key pathogen-regulatory host factors present within the individual GO class-specific modules, delineation of the transcriptionally coregulated clusters would define how the functioning of each of these modules was influenced by the infection. Such an analysis proved fruitful as it revealed the topological shifts that were induced in the

subnetworks, to bias toward a favorable outcome for the pathogen. This was typified by observed modulation of the immune/inflammation/stress subnetwork wherein suppression of inflammatory response mediators was further exacerbated through a concomitant induction of anti-inflammatory and other immunosuppressive molecules. In a similar vein, the targeted regulation of enzymes within the lipid metabolism module is also expected to contribute toward pathogen sustenance by promoting a nutritive environment and/or providing an additional route to the manipulation of macrophage innate immune responses (Gutierrez et al., 2009; Schaible and Kaufmann, 2005). Significantly, over half of the validated targets identified by our siRNA screen were also transcriptionally modulated, suggesting a proactive control by Mtb over at least some of the host factors that are critical for its survival. Thus, these collective results provide a snapshot of the calibration in functioning of the individual host cell modules that the pathogen enforces as its survival strategy. A detailed analysis of the coregulated pathways should clearly yield a more global perspective on pathogen-induced regulation of host cell responses.

The phenotypic and genotypic diversifications exhibited by most, if not all, pathogens clearly represent diverse adaptation mechanisms that are engendered in the context of the target host population. However, the question of whether and how such adaptations translate at the level of redefining the dynamics of host-pathogen interactions has remained unanswered. At least as shown here for Mtb, this question appears to be particularly relevant for understanding the variability of mechanisms that can support the virulence properties of the pathogen. This was exemplified by the panel of field isolates tested, where each member depended upon a unique spectrum of host molecules for its intracellular persistence. These differences were primarily guided by distinctions in clade identity, though lesser contributions due to phenotypic variations are also likely. However, such differences notwithstanding, the distribution of Mtb strain-specific host factors between the modules describing diverse cellular functions remained relatively constant. This implies that regardless of the Mtb genotype or phenotype, establishment of a successful infection involves an obligatory dependence on the spectrum of cellular activities represented by these modules.

A particular highlight of our experiments comparing different clinical isolates was the identification of a subset of 74 host proteins whose presence constituted an invariant requirement for optimal survival of all Mtb strains tested. That is, this subset defined an obligate survival axis for Mtb that was resistant to at least the range of adaptive variations of pathogen that were explored in this study. The functional attributes of this axis could be further resolved by our discovery that over half of its constituents acted through the regulation of autophagy. These findings underscore the idea that regardless of the broad spectrum of variants that Mtb exhibits in the human population, its persistence in the host cellular environment predominantly hinges on its ability to modulate the process of autophagy. Further, our subsequent results both from experiments examining synergy with IFNγ and from a pathway mapping exercise support the idea that these mediators collectively interfere at multiple stages of the autophagy-inducing pathways.

Thus, in summary, our present detailing of host molecules involved during the stabilization of Mtb infection provides insight into the molecular mechanisms that facilitate persistence of pathogen in the host cell. Further, although we detected divergence in pathogenetic mechanisms being exploited by distinct field isolates, the invariant host-specific components of this interplay could nonetheless be successfully captured. Of special emphasis in this regard is our subsequent delineation that the majority of these latter components constituted regulatory components of a common antimicrobial module of the host cell. We believe that this finding has important implications, given that an additional avenue for long-term persistence of mycobacteria in the host cell likely involves a stochastic distribution of its population between various intracellular niches (Young et al., 2008). Under such circumstances, then, autophagy provides a unifying mechanism by which each of these individual subpopulations can simultaneously be eliminated. Finally, we also note a natural corollary of these observations that several of the host factors identified here also provide attractive targets for the development of drugs against tuberculosis.

EXPERIMENTAL PROCEDURES

A detailed description of the methodologies employed for various aspects of this study and the optimization experiments for arriving at the screening procedure are provided in the Extended Experimental Procedures. All experiments with *M. tuberculosis* were approved by the Institutional Biosafety Committee and performed in a biosafety level III facility. The isolates BND320, BND433, JAL2261, and JAL2287 were a kind gift from V.M. Katoch (National Jalma Institute for Leprosy and other Mycobacterial Diseases), and the spoligotyping results of all the isolates used here was provided by S. Kulkarni (Bhabha Atomic Research Centre[BARC]).

siRNA Library

Dharmacon siGENOME SMARTpool siRNA Library for the complete human genome comprising of 18,174 targets was procured from Thermo Scientific. The SMARTpool library consists of a pool of four different oligos for each target gene. For validation studies, all the four oligos for each genes used in the first library were procured separately and tested individually.

Infection of Cells and the siRNA Screen

THP-1 cells were cultured in RPMI 1640 (GIBCO Laboratories) supplemented with 10% FCS (Hyclone) and were maintained between 2×10^5 and 10×10^5 cells per ml at 37°C in a humidified, 5% CO_2 atmosphere. Before infection, cells were plated in 96 well plates at 1×10^4 cells per well and differentiated with PMA (5 ng/ml) for a period of 24 hr. The detailed procedure for infection of cells, the siRNA screen, and analysis of the resultant data is described in the Extended Experimental Procedures. CFUs were calculated from the actual colony counts obtained. Counts were multiplied with the dilution factor and the volume of the diluted sample used for plating. CFU values were expressed on a per ml basis.

RNA Isolation and Microarray Analysis

RNA was isolated from either uninfected THP-1 cells or cells infected with H37Rv for 16, 48, 90 hr. A one-color microarray-based gene expression analysis was performed by hybridization against a human whole-genome array consisting of probes for 44,000 genes (Agilent). For each time point, the hybridization was performed on duplicate sets of cells. For uninfected cells, we used A/P calls as an indicator of the presence of a given transcript. To define alterations in the level of a given transcript after infection, we considered a gene to be upregulated if the signal log ratio between the infected and the uninfected sample was higher than 1 (>2-fold increase) and the detection p value of the infected sample was higher than 0.95. Similarly, a gene was considered to

be downregulated if the signal log ratio was less than −1 (>2-fold decrease) and the detection p value of the reference sample was higher than 0.95. Further, only those genes that presented a consistent change in both the biological repeats were taken as being differentially expressed. The results of our microarray analysis are available in the GEO repository (accession number GSE19052).

Extraction of the Mtb-Regulatory Network and Its Analysis

Host-specific targets validated by our siRNA screen were used to build the Mtb-regulatory network. Each of these 275 molecules was individually searched in the STRING database (http://string.embl.de/) for its functional associations. STRING is a database of both known and predicted protein-protein interactions. These include direct (physical) and indirect (functional) associations, which are derived from four separate sources: genomic context, high-throughput experiments, coexpression, and prior knowledge. We selected all interactions/associations available for a given node showing a combined score of more than 0.7. The scores given in the STRING database define the confidence limit for each described interaction/association. A combined score of 0.7 is recommended as the high stringency criterion by the database. The functional associations identified for all of the molecules were then merged together and imported into Cytoscape 2.6.1 as a two-column network (Mtb-regulatory network).

GO analysis of the Mtb-regulatory network was performed with the Bingo 2.3 plugin in Cytoscape 2.6.1. Only categories with a very low p value ($<10^{-5}$) were considered as enriched in the network as determined by Hypergeometric statistical test employing the Benjamini and Hochberg false discovery rate correction (Maere et al., 2005).

ACCESSION NUMBERS

The GEO accession number for the gene expression analysis reported in this paper is GSE19052.

SUPPLEMENTAL INFORMATION

Supplemental Information includes Extended Experimental Procedures, four figures, and ten tables and can be found with this article online at doi:10.1016/j.cell.2010.02.012.

ACKNOWLEDGMENTS

This study was funded in part by the Department of Biotechnology, Government of India, and in part by the Institute of Life Sciences, Hyderabad. We are grateful to V. Biswas, M. Jain, N. Karwal, R. Kashikar, S. Kumari, A. Kumar, K. Midha, M.K. Midha, S. Seth, S. Sharma, M. Sharma, Z. Sidiqui, A. Srivastava, and S. Tirpattiwar for technical assistance during the various stages of the RNA interference screen. We also thank S. Kulkarni (BARC) for spoligotyping analysis of the field isolates used in this study.

Received: May 29, 2009
Revised: October 2, 2009
Accepted: February 8, 2010
Published: March 4, 2010

REFERENCES

Barabási, A.L., and Oltvai, Z.N. (2004). Network biology: understanding the cell's functional organization. Nat. Rev. Genet. *5*, 101–113.

Brudey, K., Driscoll, J.R., Rigouts, L., Prodinger, W.M., Gori, A., Al-Hajoj, S.A., Allix, C., Aristimuño, L., Arora, J., Baumanis, V., et al. (2006). Mycobacterium tuberculosis complex genetic diversity: mining the fourth international spoligotyping database (SpolDB4) for classification, population genetics and epidemiology. BMC Microbiol. *6*, 23.

Davila, S., Hibberd, M.L., Hari Dass, R., Wong, H.E., Sahiratmadja, E., Bonnard, C., Alisjahbana, B., Szeszko, J.S., Balabanova, Y., Drobniewski, F., et al. (2008). Genetic association and expression studies indicate a role of toll-like receptor 8 in pulmonary tuberculosis. PLoS Genet. *4*, e1000218.

de Chastellier, C. (2009). The many niches and strategies used by pathogenic mycobacteria for survival within host macrophages. Immunobiology, in press. Published online March 2, 2009.

Flynn, J.L. (1999). Why is IFN-gamma insufficient to control tuberculosis? Trends Microbiol. *7*, 477–478, author reply 478–479.

Flynn, J.L., and Chan, J. (2001). Immunology of tuberculosis. Annu. Rev. Immunol. *19*, 93–129.

Fratti, R.A., Chua, J., Vergne, I., and Deretic, V. (2003). Mycobacterium tuberculosis glycosylated phosphatidylinositol causes phagosome maturation arrest. Proc. Natl. Acad. Sci. USA *100*, 5437–5442.

Gagneux, S., DeRiemer, K., Van, T., Kato-Maeda, M., de Jong, B.C., Narayanan, S., Nicol, M., Niemann, S., Kremer, K., Gutierrez, M.C., et al. (2006). Variable host-pathogen compatibility in Mycobacterium tuberculosis. Proc. Natl. Acad. Sci. USA *103*, 2869–2873.

Gertow, K., Pietiläinen, K.H., Yki-Järvinen, H., Kaprio, J., Rissanen, A., Eriksson, P., Hamsten, A., and Fisher, R.M. (2004). Expression of fatty-acid-handling proteins in human adipose tissue in relation to obesity and insulin resistance. Diabetologia *47*, 1118–1125.

Ginsberg, A.M., and Spigelman, M. (2007). Challenges in tuberculosis drug research and development. Nat. Med. *13*, 290–294.

Gutierrez, M.G., Master, S.S., Singh, S.B., Taylor, G.A., Colombo, M.I., and Deretic, V. (2004). Autophagy is a defense mechanism inhibiting BCG and Mycobacterium tuberculosis survival in infected macrophages. Cell *119*, 753–766.

Gutierrez, M.G., Gonzalez, A.P., Anes, E., and Griffiths, G. (2009). Role of lipids in killing mycobacteria by macrophages: evidence for NF-kappaB-dependent and -independent killing induced by different lipids. Cell. Microbiol. *11*, 406–420.

Jain, M., Petzold, C.J., Schelle, M.W., Leavell, M.D., Mougous, J.D., Bertozzi, C.R., Leary, J.A., and Cox, J.S. (2007). Lipidomics reveals control of Mycobacterium tuberculosis virulence lipids via metabolic coupling. Proc. Natl. Acad. Sci. USA *104*, 5133–5138.

Kaufmann, S.H., Cole, S.T., Mizrahi, V., Rubin, E., and Nathan, C. (2005). Mycobacterium tuberculosis and the host response. J. Exp. Med. *201*, 1693–1697.

Koul, A., Herget, T., Klebl, B., and Ullrich, A. (2004). Interplay between mycobacteria and host signalling pathways. Nat. Rev. Microbiol. *2*, 189–202.

Kuijl, C., Savage, N.D., Marsman, M., Tuin, A.W., Janssen, L., Egan, D.A., Ketema, M., van den Nieuwendijk, R., van den Eeden, S.J., Geluk, A., et al. (2007). Intracellular bacterial growth is controlled by a kinase network around PKB/AKT1. Nature *450*, 725–730.

Levine, B., and Deretic, V. (2007). Unveiling the roles of autophagy in innate and adaptive immunity. Nat. Rev. Immunol. *7*, 767–777.

MacMicking, J.D., Taylor, G.A., and McKinney, J.D. (2003). Immune control of tuberculosis by IFN-gamma-inducible LRG-47. Science *302*, 654–659.

Maere, S., Heymans, K., and Kuiper, M. (2005). BiNGO: a Cytoscape plugin to assess overrepresentation of gene ontology categories in biological networks. Bioinformatics *21*, 3448–3449.

Monack, D.M., Mueller, A., and Falkow, S. (2004). Persistent bacterial infections: the interface of the pathogen and the host immune system. Nat. Rev. Microbiol. *2*, 747–765.

Nau, G.J., Richmond, J.F., Schlesinger, A., Jennings, E.G., Lander, E.S., and Young, R.A. (2002). Human macrophage activation programs induced by bacterial pathogens. Proc. Natl. Acad. Sci. USA *99*, 1503–1508.

Pandey, A.K., and Sassetti, C.M. (2008). Mycobacterial persistence requires the utilization of host cholesterol. Proc. Natl. Acad. Sci. USA *105*, 4376–4380.

Park, J.S., Tamayo, M.H., Gonzalez-Juarrero, M., Orme, I.M., and Ordway, D.J. (2006). Virulent clinical isolates of Mycobacterium tuberculosis grow rapidly and induce cellular necrosis but minimal apoptosis in murine macrophages. J. Leukoc. Biol. *79*, 80–86.

Schaible, U.E., and Kaufmann, S.H. (2005). A nutritive view on the host-pathogen interplay. Trends Microbiol. *13*, 373–380.

Seglen, P.O., and Gordon, P.B. (1982). 3-Methyladenine: specific inhibitor of autophagic/lysosomal protein degradation in isolated rat hepatocytes. Proc. Natl. Acad. Sci. USA *79*, 1889–1892.

Singh, S.B., Davis, A.S., Taylor, G.A., and Deretic, V. (2006). Human IRGM induces autophagy to eliminate intracellular mycobacteria. Science *313*, 1438–1441.

Theus, S.A., Cave, M.D., Eisenach, K., Walrath, J., Lee, H., Mackay, W., Whalen, C., and Silver, R.F. (2006). Differences in the growth of paired Ugandan isolates of Mycobacterium tuberculosis within human mononuclear phagocytes correlate with epidemiological evidence of strain virulence. Infect. Immun. *74*, 6865–6876.

Ting, L.M., Kim, A.C., Cattamanchi, A., and Ernst, J.D. (1999). Mycobacterium tuberculosis inhibits IFN-gamma transcriptional responses without inhibiting activation of STAT1. J. Immunol. *163*, 3898–3906.

van der Wel, N., Hava, D., Houben, D., Fluitsma, D., van Zon, M., Pierson, J., Brenner, M., and Peters, P.J. (2007). M. tuberculosis and M. leprae translocate from the phagolysosome to the cytosol in myeloid cells. Cell *129*, 1287–1298.

Van Limbergen, J., Stevens, C., Nimmo, E.R., Wilson, D.C., and Satsangi, J. (2009). Autophagy: from basic science to clinical application. Mucosal Immunol *2*, 315–330.

Vergne, I., Chua, J., Singh, S.B., and Deretic, V. (2004). Cell biology of mycobacterium tuberculosis phagosome. Annu. Rev. Cell Dev. Biol. *20*, 367–394.

Warner, D.F., and Mizrahi, V. (2007). The survival kit of Mycobacterium tuberculosis. Nat. Med. *13*, 282–284.

Young, D., Stark, J., and Kirschner, D. (2008). Systems biology of persistent infection: tuberculosis as a case study. Nat. Rev. Microbiol. *6*, 520–528.